Hindawi
Advances in Civil Engineering
Volume 2021, Article ID 6674195, 13 pages
https://doi.org/10.1155/2021/6674195

Research Article

Stability Analysis on the Long-Term Operation of the Horizontal Salt Rock Underground Storage

Chengzhong Zhang,[1,2] **Qiang Zhang**,[1,2] **Weiwei Li**,[3] **Zhanping Song**,[1,2] **and Junbao Wang**[1,2]

[1]*School of Civil Engineering, Xi'an University of Architecture and Technology, Xi'an, Shaanxi 710055, China*
[2]*Shaanxi Key Laboratory of Geotechnical and Underground Space Engineering, Xi'an 710055, China*

Correspondence should be addressed to Qiang Zhang; nndsjyzq@163.com and Weiwei Li; 1278040448@qq.com

Received 26 November 2020; Revised 23 December 2020; Accepted 2 January 2021; Published 15 January 2021

Academic Editor: Song-He Wang

The construction of the vertical cavern in the salt dome deposit can meet the requirements of both storage capacity and tightness. However, if the vertical cavern is still used as the design shape of the salt rock underground storage in the layered salt rock deposit, the high design capacity cannot be guaranteed while the tightness is satisfied. In this case, the use of a large-span horizontal cavern as the design shape of the salt rock storage can not only effectively increase the design capacity of the storage, but also solve the problems such as the stability and tightness of the storage during the operation period by improving the structural form and working mode. Based on this, the ellipsoid-shaped horizontal salt rock underground storage is taken as an example, and a single-cavern horizontal salt rock underground storage model with different diameter-to-height ratios is established by using FLAC^{3D} software. The change law of vertical and horizontal displacements, volume loss rate, and plastic zone distribution of salt rock storage changing with the diameter-to-height ratio are studied, and the optimal diameter-to-height ratio is determined. And then the long-term operation process of the double-cavern horizontal salt rock underground storage under the optimal diameter-to-height ratio is simulated, and the optimal pillar width is obtained.

1. Introduction

Energy (oil and natural gas) is the material basis for the survival and development of human society, occupying an important strategic position in the national economy [1–3]. However, energy reserves in China are relatively small and extremely dependent on foreign countries. The energy problems are getting worse. Due to the obvious increase in international trade disputes and unstable factors in major energy regions, international energy supply will inevitably be interrupted, posing a serious threat to energy import security [4–7]. In order to ensure the sustainable and healthy development of the national economy and energy security, the construction of underground energy storage is extremely urgent [8–11].

With the large-scale construction and operation of salt rock underground storage, how to improve the effective storage capacity of salt rock underground storage and ensure the safety and stability of its long-term operation has become a hot issue of current research [12–15]. In recent years, related scholars have conducted a large number of in-depth studies on the stability of salt rock underground storage from the aspects of influencing factors and stability evaluation [16–20]. Xing et al. [21] conducted numerical simulation analysis on the long-term stability of salt rock underground storage with different sizes and different minimum internal pressures from the aspects of convergence, damage, dilatancy ratio, and effective strain. Liang et al. [22] studied the variation law of indexes such as volume shrinkage rate and surrounding rock safety coefficient of salt rock underground storage under different operation pressures by using FLAC^{3D} software. Wang et al. [23] selected factors such as deformation, plastic zone development, effective strain, safety coefficient, and volumetric shrinkage as

indicators to evaluate the influence of the spacing between new and old caverns on the stability of salt rock underground storage. Mortazavi and Nasab [24] studied the influence of cavern size, buried depth, salt rock deformation modulus, and in situ stress state on the stability of large salt rock underground storage. Khaledi et al. [25] studied the change rules of volume convergence, damage expansion, and permeability of salt rock underground storage during the construction and operation period using the elastic-viscoplastic creep model. Based on the statistical results of global salt rock mining accidents, Zhang et al. [26] used the fault tree model to analyze and identify the factors that lead to oil and gas leakage, surface settlement, and cavern group destruction and established a comprehensive risk probability evaluation method and risk grading standard for salt rock underground storage caverns. On the basis of the existing design and stability analysis criteria and methods for salt rock underground storage, Habibi [27] proposed stress-based and damage-based stability analysis criteria for salt rock underground storage. Liu et al. [28] contrasted and analyzed the stability of four typical cavern shapes of salt rock underground storage using the numerical simulation method. The results showed that the ellipsoidal cavern has the best stability, while the cylindrical cavern and the cuboid cavern have the worst stability. Deng et al. [29] analyzed the time-dependent deformation and long-term stability of salt rock underground storage by introducing nonlinear viscoelastic, viscoplastic, and viscous damage models into the deformation strengthening theory. Wang and Liu [30] studied the influence of the existence of interlayers on the long-term stability of salt rock underground storage by using three different mechanical instability criteria and calculated the limit radius of interlayers under different criteria. Zhang et al. [31] established the roof leakage model of the salt rock underground storage by Comsol software and analyzed the leakage range and saltwater leakage at different times and the safety problems caused by it. Based on the major accidents in the global salt rock underground storage, Yang et al. [32] established a comprehensive evaluation method for major risk losses based on the analytic hierarchy process, providing a theoretical basis for the evaluation and prevention of major risks in the construction and operation of salt rock underground storage. Chen et al. [33] studied the influence of gas pressure and the ratio of long and short axes on the stability of double-cavern salt rock underground storage with small spacing by using numerical simulation methods. The results showed that gas pressure has a significant effect on the stability of underground salt rock storage, while the ratio of long axis to short axis has an important impact on the volume loss rate and roof settlement of underground salt rock storage. At present, relevant scholars have carried out more in-depth research on the long-term stability of salt rock underground storage, and most of their research objects are vertical salt rock storage (the height of the storage is greater than the maximum cavern diameter). However, because the layered salt rock deposit is characterized by many layers and small single-layer thickness, under the same geological conditions, the effective capacity of the horizontal salt rock underground storage with a large span is higher than that of the vertical salt rock underground storage [34–38]. There are relatively few studies on the long-term stability of horizontal salt rock underground storage. It is necessary to conduct an in-depth study on the feasibility and long-term stability of the establishment of horizontal salt rock underground storage [39–41].

The ellipsoidal horizontal salt rock underground storage is taken as an example in this paper, and the FLAC^{3D} numerical simulation software is used to establish a single-cavern horizontal salt rock underground storage model with different diameter-to-height ratios. The change law of volumetric loss rate, stress, and plastic zone development of underground salt rock storage under different diameter-to-height ratios are studied, and the optimal diameter-to-height ratio is determined. On this basis, the long-term operation process of double-cavern horizontal salt rock underground storage is simulated numerically, and the optimal pillar width is obtained.

2. Physical Mechanics Model

2.1. Cavern Shape. At present, most of the salt rock underground storage in operation and under construction at home and abroad are vertical caverns with relatively large height-to-diameter ratios. The construction of the vertical cavern in a salt dome deposit can meet the higher requirement of storage capacity and tightness. However, for the layered salt rock deposits with many layers and small single-layer thickness, the vertical cavern as the design shape of the salt rock storage can not achieve high storage design capacity while meeting the tightness of the storage. In this case, adopting the horizontal cavern with a large span as the design shape of salt rock underground storage can not only effectively improve the design capacity of the storage, but also solve the problems such as the stability and tightness of the storage during the operation period by improving the structural form and working mode of the storage. However, there are relatively few studies on the long-term stability of horizontal salt rock underground storage. Therefore, the long-term stability of the ellipsoidal horizontal salt cavern (as shown in Figure 1) is analyzed using the FLAC^{3D} software in this paper.

2.2. Geological Conditions. According to the distribution characteristics of layered salt rock deposits, it is assumed that the stratum is as follows: the buried depth of the salt rock layer is 800~920 m and the upper and lower layers of salt rock are mudstone.

Take the height of the salt rock underground storage $h = 2a = 60$ m and reserve 30 m at the top and bottom of the salt rock layer to ensure the tightness of the salt rock storage. In the numerical simulation, the self-weight stress of the stratum within 500 m below the ground surface is simplified into a uniformly distributed load of 14 MPa and applied to the top of the numerical model (as shown in Figure 2). Apply normal constraints on the front, back, left, right, and bottom of the model, namely, constraints in the x, y, and negative z directions. The dimensions of the model in the x, y, and z directions are 800 m, 800 m, and 700 m, respectively.

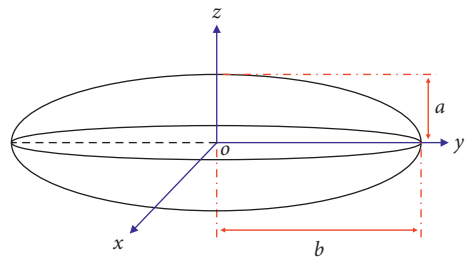

Figure 1: Schematic diagram of ellipsoidal horizontal salt rock cavern (a and b are the radius of the minor axis and the major axis, resp.).

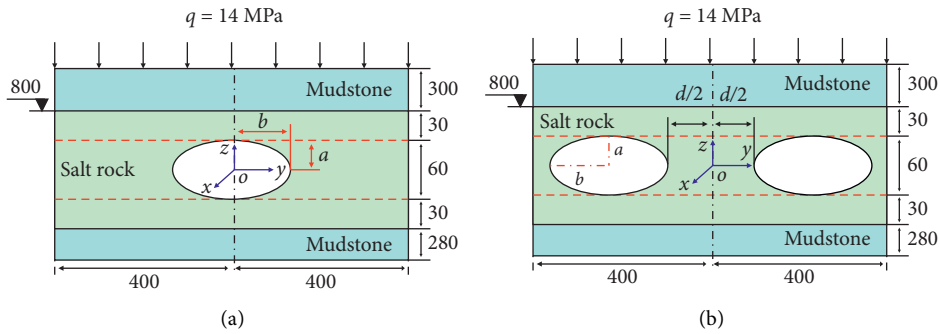

Figure 2: Schematic diagram of the numerical model of horizontal salt rock storage (unit: m). (a) Single cavern and (b) double cavern.

2.3. Mechanical Parameters. The numerical model of salt rock underground storage established in this paper involves two rock materials: salt rock and mudstone. The Cpower model and the Mohr–Coulomb model are selected as the constitutive models of the salt rock and mudstone. The basic mechanical parameters and model parameters of these two kinds of rocks are shown in Table 1 [42, 43].

3. Stability Analysis of Single-Cavern Horizontal Salt Rock Underground Storage

It can be seen from 2.2 that the height of the salt rock underground storage is 60 m; that is, the minor axis radius a is 30 m, and it is necessary to determine the diameter in the horizontal direction, that is, the size of the major axis radius b. If the span of the storage in the horizontal direction is too small, it is not economical. If the span of the storage is too large in the horizontal direction, it will be detrimental to the stability of the storage. Therefore, in this section, four single-cavern horizontal salt rock underground storage models with different diameter-to-height ratios ($N = 1.5$, 2.0, 2.5, and 3.0) have been established to analyze the influence of the diameter-to-height ratio on its long-term stability.

Considering that the numerical model of the single-cavern horizontal salt rock underground storage is symmetric about the xoz plane and the yoz plane, in order to simplify the workload and improve the computational efficiency, only a 1/4 model is established (as shown in Figure 3). For traditional salt rock underground storage, most of them are in the form of a single well and single pipe structure. For the structure, its operation process includes four stages: constant high pressure, gas production depressurization, constant low pressure, and gas injection pressurization. This will inevitably cause the salt rock underground storage to be under cyclic loading, threatening its safety. In order to keep the salt rock underground storage under constant pressure during operation and ensure the working efficiency of the storage, relevant scholars optimized the traditional structure form of the salt rock underground storage and put forward a two-well and two-pipe structure. In order to ensure the tightness of the underground salt rock storage, its maximum operation internal pressure generally does not exceed 80% of the overlying formation pressure. Therefore, the operation internal pressure selected in the numerical simulation of this section is 16 MPa. Table 2 shows the model parameters under 4 different working conditions.

3.1. Vertical and Horizontal Displacement. Figure 4 shows the vertical displacement cloud map of the surrounding rock of a single-cavern horizontal salt rock underground storage (diameter-to-height ratio $N = 2.5$) after operation for $5a$, $10a$, $15a$, and $20a$. It can be seen that during the long-term operation of the single-cavern horizontal salt rock underground storage, the displacement distribution of the surrounding rocks on the left and right sides is relatively even. The displacement distribution of the upper and lower surrounding rocks is more concentrated, and the top settlement value is greater than the bottom uplift value. When the diameter-to-height ratio $N = 2.5$, the maximum settlement at the top and the maximum uplift at the bottom of the salt rock storage after $20a$ of operation are 1.3220 m and 0.9706 m, respectively. Through analysis, it can be seen that when the diameter-to-height ratio $N = 1.5$, 2.0, and 3.0, the vertical displacement

Table 1: Basic mechanical parameters of salt rock and mudstone.

Parameters	Elastic modulus (GPa)	Poisson's ratio	Cohesion (MPa)	Internal friction (°)	Tensile strength (MPa)	Density ($g \cdot cm^{-3}$)	A ($MPa^{-3} \cdot h^{-1}$)	n
Salt rock	3.00	0.30	10.00	21.72	1.0	2.14	$8.48e-9$	3
Mudstone	10.18	0.23	15.63	35.00	2.2	2.60	—	—

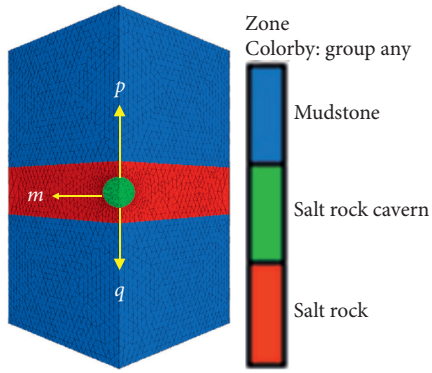

Figure 3: Numerical model of single-cavern horizontal salt rock underground storage ($N = 1.5$).

distribution of surrounding rock in the salt rock storage changing with time is basically consistent with that of salt rock storage when diameter-to-height ratio $N = 2.5$.

Figure 5 shows the vertical displacement cloud map of the surrounding rock after operation for 20a of the salt rock storage when diameter-to-height ratio $N = 1.5$, 2.0, and 3.0. It can be seen from Figures 4(d) and 5 that when the operation time is the same, the vertical displacement of the surrounding rock of the storage gradually increases with the increase of the diameter-to-height ratio. Through analysis, it can be found that when the diameter-to-height is relatively small ($N = 1.5$), the maximum settlement of the surrounding rock of the salt rock storage basically occurs at the highest point of the storage. As the diameter-to-height ratio increases, the location of the maximum settlement gradually shifts to both sides of the vault. When $N = 1.5$, the horizontal distance between the position where the maximum settlement occurs and the center position of the upper part of the salt rock storage (point p in Figure 3) is $L_1 = 17.6$ m. The horizontal distance between the location of the largest uplift and the lower center of the salt rock storage (point q in Figure 3) is $L_2 = 11.8$ m. In addition, when $N = 2.0$, 2.5, and 3.0, the values of L_1 are 35.7 m, 50.9 m, and 59.5 m, respectively, and the values of L_2 are 28.7 m, 42.7 m, and 59.5 m, respectively.

Figure 6 shows the variation of the vertical displacement of point p and point q with the operation time of the salt rock underground storage. It can be seen from Figure 6(a) that, during the operation of the horizontal salt rock underground storage, the arch settlement (vertical displacement of point p) increases continuously with the increase of the operation time. In the early stage of storage, the arch settlement develops rapidly. With the increase of operation time, the development rate of arch settlement decreases gradually. After the operation time exceeds 3a, the arch settlement increases linearly with the operation time. It can be seen from Figure 6(b) that, during the operation of the horizontal salt rock underground storage, the uplift deformation at the lowest point (point q in Figure 3) of the storage continues to increase with the extension of the operation time. In the initial stage of gas storage operation, the rate of uplift deformation is relatively fast. When the operation time exceeds 1a, the uplift deformation at the lowest point of the storage basically increases linearly with time.

Figure 7 shows the variation of the maximum vertical displacement of the roof and floor of the single-cavern horizontal salt rock underground storage with the diameter-to-height ratio. It can be seen from Figure 6(a) that, as the diameter-to-height ratio N increases, the roof settlement of the single-cavern horizontal salt rock underground storage gradually increases. The maximum roof settlement of the salt rock storage with diameter-to-height ratio $N = 1.5$, 2.0, 2.5, and 3.0 after operation for 20a is 1.2884 m, 1.3049 m, 1.3219 m, and 1.3326 m, respectively. It can be seen from Figure 6(b) that, as the diameter-to-height ratio N increases, the floor uplift of the single-cavern horizontal salt rock underground storage gradually decreases. The maximum floor uplift of the salt rock storage with diameter-to-height ratio $N = 1.5$, 2.0, 2.5, and 3.0 after operation for 20a is 1.1275 m, 1.0260 m, 0.9705 m, and 0.9242 m, respectively.

The differences of the stress state between points p and q are the main reason that resulting in the diameter-to-height ratio having the opposite effect on the roof settlement and floor uplift of the salt rock storage. The larger the diameter-to-height ratio, the larger the span of the salt rock underground storage, the greater the force on point p, and the larger the roof settlement at this point. Therefore, the roof settlement at point p increases with the increase of diameter-to-height ratio. However, with the increases of diameter-to-height ratio, the force on point q gradually transfers to both sides, and the stress at this point gradually decreases. In this condition, the floor uplift at point q decreases with the increasing of diameter-to-height ratio.

Figure 8 shows the variation of the arch horizontal displacement (point m in Figure 3) of the single-cavern horizontal salt rock underground storage with different diameter-to-height ratios N. It can be seen from Figure 8(a) that the horizontal displacement of point m gradually increases with the extension of operation time. When the diameter-to-height ratio $N = 2.5$, the horizontal displacement of the salt rock storage at point m after operation for 5a, 10a, 15a, and 20a are 0.7198 m, 1.1916 m, 1.5859 m, and 1.9417 m, respectively.

It can be seen from Figure 8(b) that the horizontal displacement of point m in the salt rock storage increases with the increase of the height-to-diameter ratio at the same operation time. The analysis shows that the horizontal

Table 2: Model parameters of single-cavern horizontal salt rock underground storage.

Working conditions	a (m)	b (m)	$N = b/a$	Design reserves ($10^5 \cdot m^3$)	Operation internal pressure (MPa)
Case 1	30	45	1.5	2.545	16
Case 2	30	60	2.0	4.524	16
Case 3	30	75	2.5	7.069	16
Case 4	30	90	3.0	10.180	16

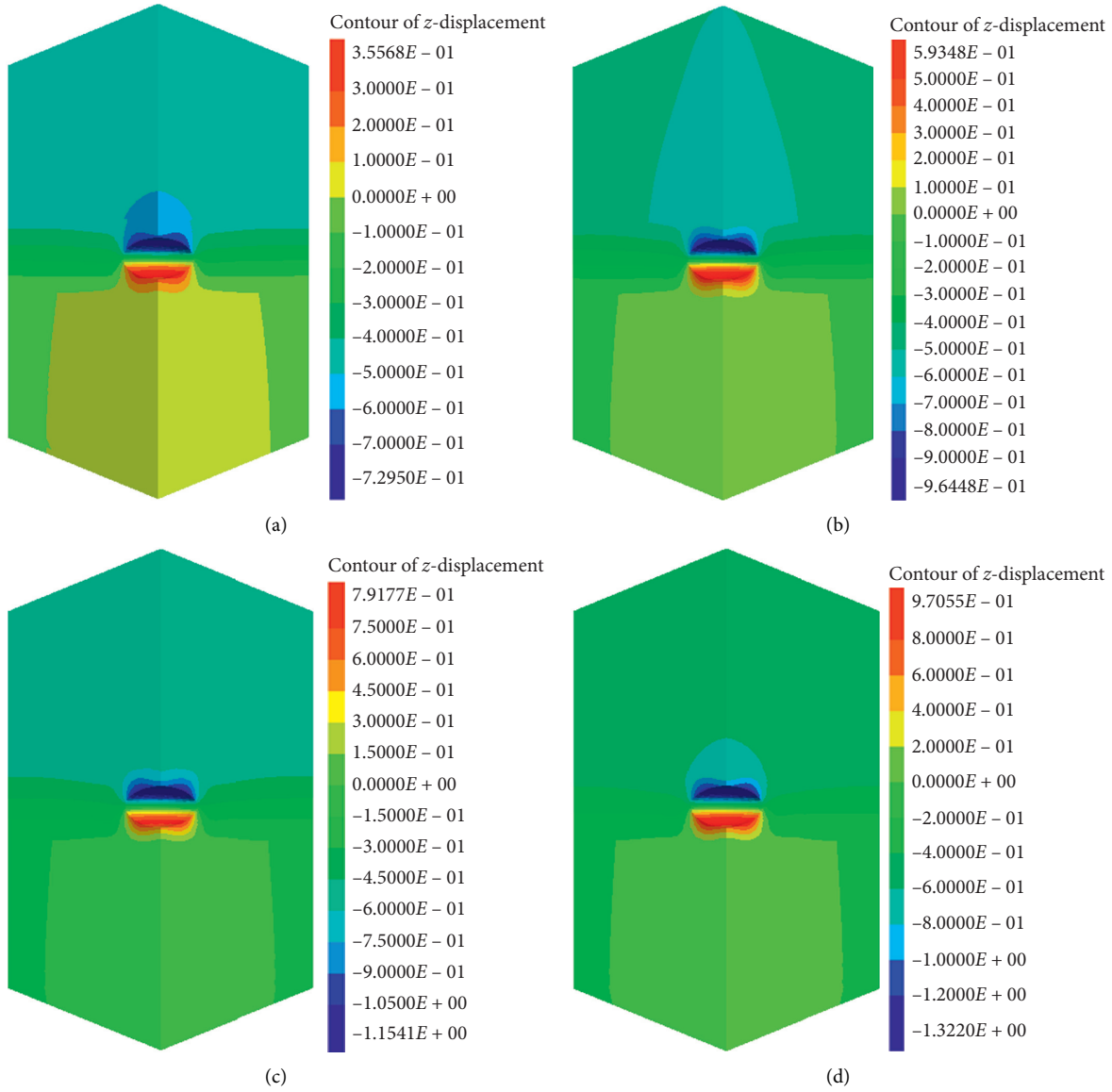

Figure 4: Cloud map of vertical displacement distribution of surrounding rock of single-cavern horizontal salt rock underground storage. (a) 5a; (b) 10a; (c) 15a; and (d) 20a.

displacements of salt rock storage with diameter-to-height ratios of 1.5, 2.0, 2.5, and 3.0 at point m after operation for 20a are 1.7245 m, 1.8386 m, 1.9417 m, and 1.9964 m, respectively.

3.2. Volume Loss Rate. It can be seen from Table 2 that the design capacities of the four horizontal salt rock underground storage with different diameter-to-height ratios simulated in this paper are $2.545 \times 10^5\ m^3$ ($N = 1.5$), $4.524 \times 10^5\ m^3$ ($N = 2.0$), $7.069 \times 10^5\ m^3$ ($N = 2.5$), and $10.180 \times 10^5\ m^3$ ($N = 3.0$). The FISH language is used to process the displacement data of the surrounding rock of the storage obtained from the numerical simulation, and the change law of the volume loss rate of the salt rock storage with operation time and diameter-to-height ratio can be obtained as shown in Figure 9.

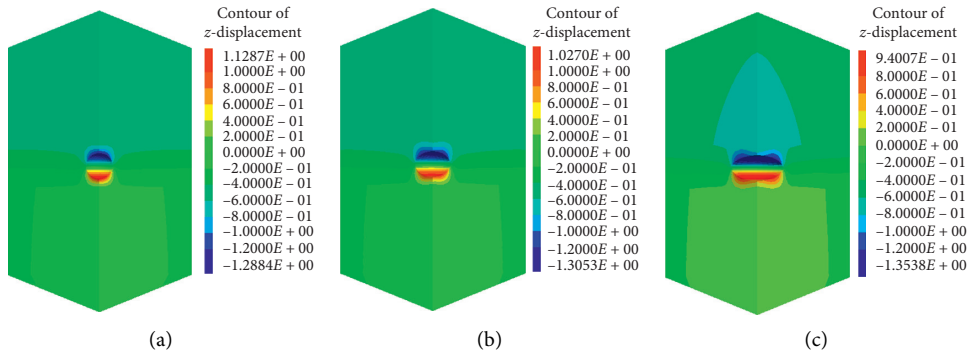

Figure 5: Cloud map of vertical displacement distribution of surrounding rock after operation for 20a of salt rock storage under different diameter-to-height ratios. (a) $N = 1.5$; (b) $N = 2.0$; and (c) $N = 3.0$.

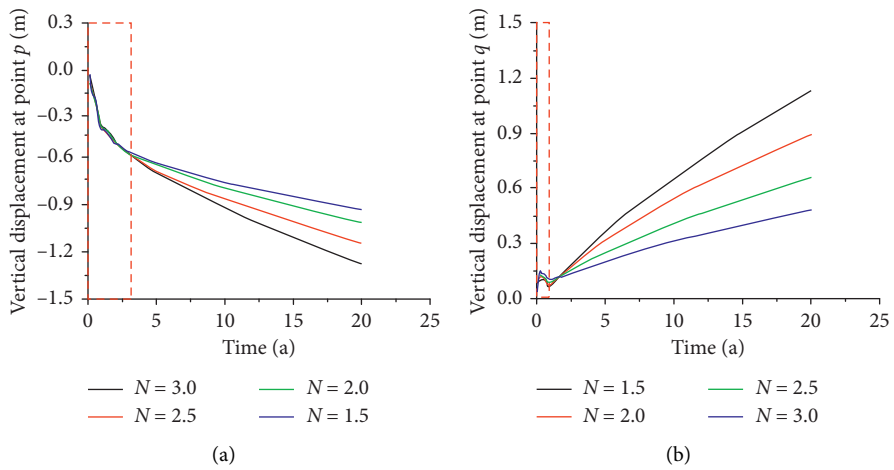

Figure 6: Vertical displacement changes at points p and q of a single-cavern horizontal salt rock underground storage. (a) Point p. (b) Point q.

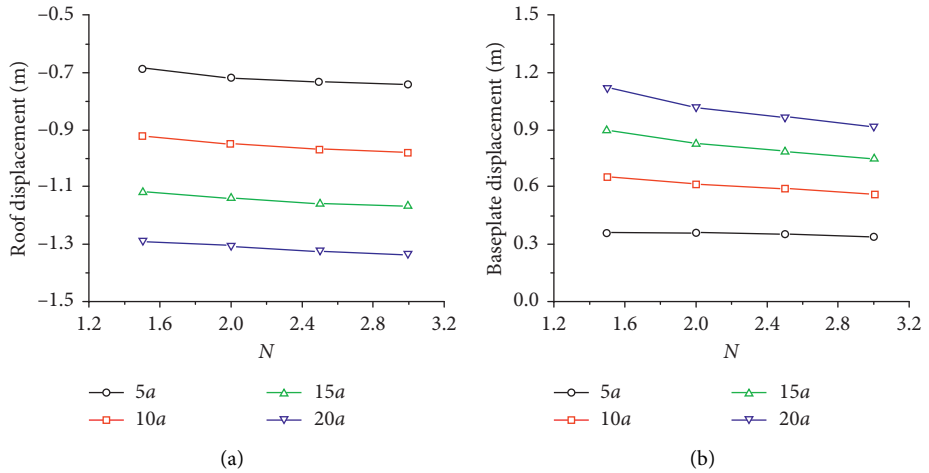

Figure 7: Variation of the maximum vertical displacement of point p and point q of a single-cavern horizontal salt rock underground storage with the diameter-to-height ratio. (a) Roof displacement. (b) Floor displacement.

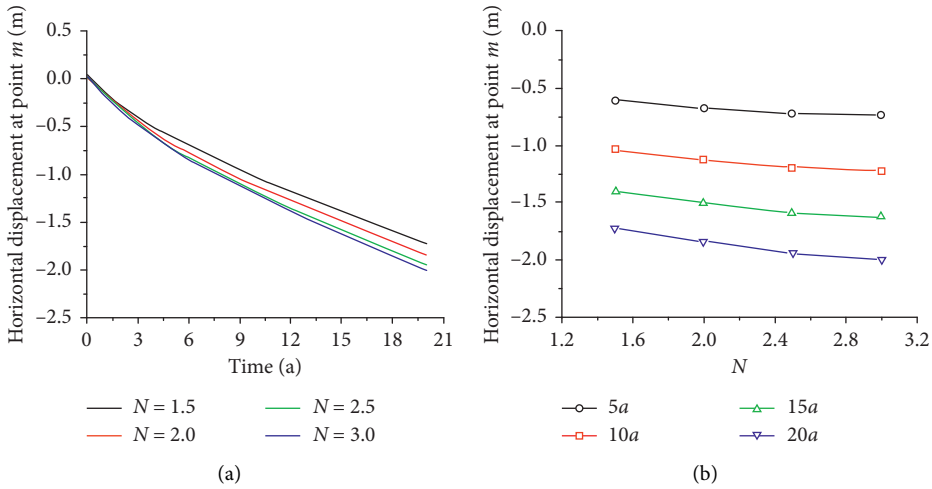

Figure 8: Variation rule of horizontal displacement at point m with operation time and diameter-to-height ratio. (a) The horizontal displacement of point m changing with operation time. (b) The horizontal displacement of point m changing with of diameter-to-height ratio.

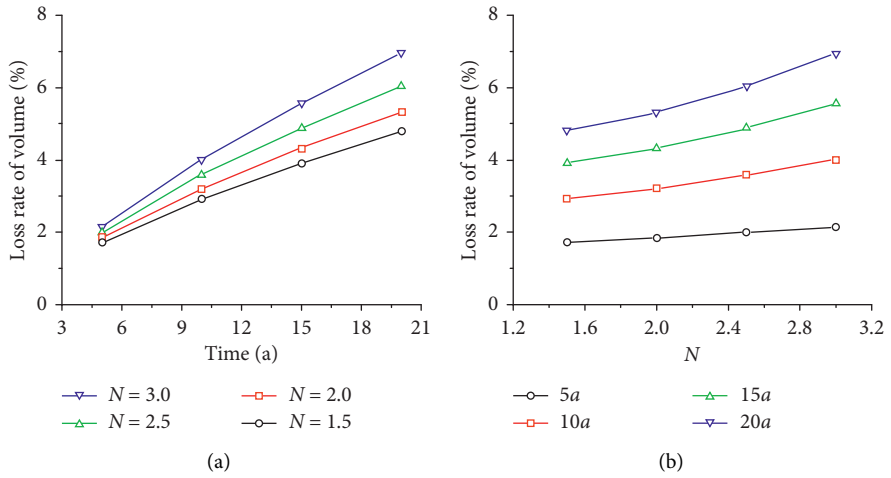

Figure 9: Variation of volume loss rate of single-cavern horizontal salt rock underground storage with operation time and diameter-to-height ratio. (a) The variation of volume loss rate with operation time. (b) The variation of volume loss rate with diameter-to-height ratio.

It can be seen from Figure 9 that the volume loss rate of the single-cavern horizontal salt rock underground storage gradually increases with the extension of the operation time and the increase of the diameter-to-height ratio. The analysis shows that when the diameter-to-height ratio $N = 1.5$, the volume loss rate of the storage after operation for $5a$ and $20a$ is 1.7090% and 4.8014%, respectively. When the diameter-to-height ratio N increases to 3.0, the volume loss rate of the storage after operation for $5a$ and $20a$ is 2.1293% and 6.9500%, respectively. It can be seen that the volume loss rates of the four single-cavern horizontal salt rock underground storage selected in this paper with different diameter-to-height ratios all meet the availability requirements; that is, the volume loss rate of storage after operation for $5a$ is less than 5%, and the volume loss rate after operation for $20a$ is less than 15%.

3.3. Plastic Zone Distribution. Figure 10 shows the change rule of the plastic zone of single-cavern horizontal salt rock underground storage when the diameter-to-height ratio is $N = 2.5$ with operation time. It can be seen that the surrounding rock of the single-cavern horizontal salt rock underground storage mainly undergoes shear failure during operation. And the plastic zone is mainly distributed on the top and bottom of the salt rock storage, and a small amount of plastic zone also appears at the interface between mudstone and salt rock.

In the early stage of operation, the composition of the plastic zone of the surrounding rock of the salt rock storage is relatively complex. With the extension of the operation time, the plastic zone gradually develops. After operation for $15a$, the plastic zone basically does not change. Through analysis, it can be seen that the change rule of the plastic zone

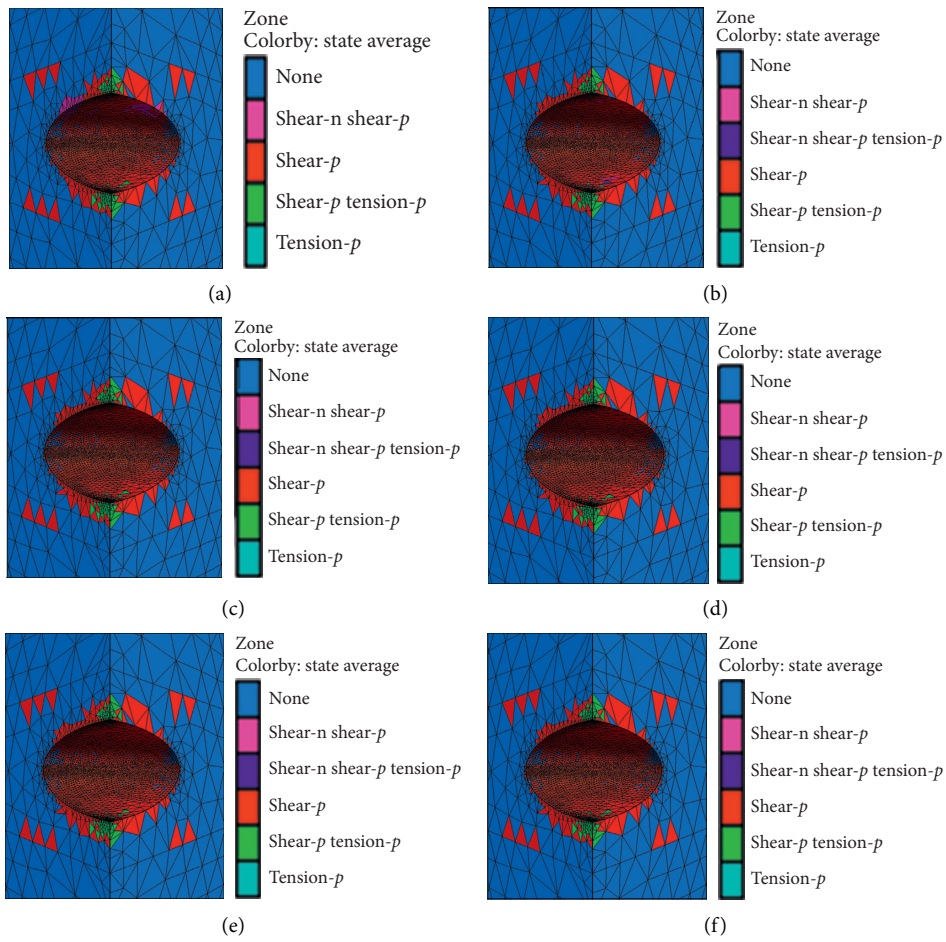

Figure 10: Variation of plastic zone of single-cavern horizontal salt rock underground storage when diameter-to-height ratio is $N = 2.5$ with operation time. (a) $1a$; (b) $3a$; (c) $5a$; (d) $10a$; (e) $15a$; and (f) $20a$.

of salt rock storage with operation time when the diameter-to-height ratio $N = 1.5$, 2.0, and 3.0 is consistent with that of the plastic zone of salt rock storage when diameter-to-height ratio $N = 2.5$.

Figure 11 shows the plastic zone distribution cloud map of the single-cavern horizontal salt rock underground storage after operation for $20a$ with different diameter-to-height ratios of $N = 1.5$, 2.0, and 3.0. It can be seen that when the diameter-to-height ratio is relatively small ($N = 1.5$ and 2.0), the plastic zone is small and mainly concentrated at the top and bottom of the storage. When the diameter-to-height ratio is relatively large ($N = 2.5$ and 3.0), the plastic zone gradually increases, and there are also plastic zones at the interface between mudstone and salt rock. In general, after operation for 20 years, the plastic zone of the salt rock storage with diameter-to-height ratios $N = 1.5$, 2.0, and 2.5 has basically stabilized. However, when the diameter-to-height ratio is $N = 3.0$, the plastic zone of the surrounding rock of the salt rock storage is still developing and has the risk of penetrating the whole salt rock layer.

From the above analysis, the smaller the diameter-to-height ratio, the smaller the volume loss rate, and the smaller the volume of the plastic zone. Thus, for the perspectives of the volume loss rate and plastic zone distribution, the smaller the diameter-to-height ratio, the better the stability of the salt rock underground storage. However, the smaller the diameter-to-height ratio, the lesser the storage capacity. Therefore, for the perspectives of storage capacity, the larger the diameter-to-height ratio of the salt rock underground storage, the higher the economy. Considering the long-term stability and economy of salt rock underground storage comprehensively and referring to the relevant engineering experience all over the world, the value of the diameter-to-height ratio of the single-cavern horizontal salt rock storage can be $N = 2.5$.

4. Stability Analysis of Double-Cavern Horizontal Salt Rock Underground Storage

In Section 3, the optimal diameter-to-height ratio ($N = 2.5$) of single-cavern horizontal salt rock underground storage is given. However, in the actual construction of salt rock underground storage, most of them adopt the form of double or multicavern to improve the gas storage capacity. And the distance between the storage should be considered to ensure its stability and safety. This section mainly takes the double-cavern horizontal salt rock underground storage with diameter-to-height ratio $N = 2.5$ as the research object

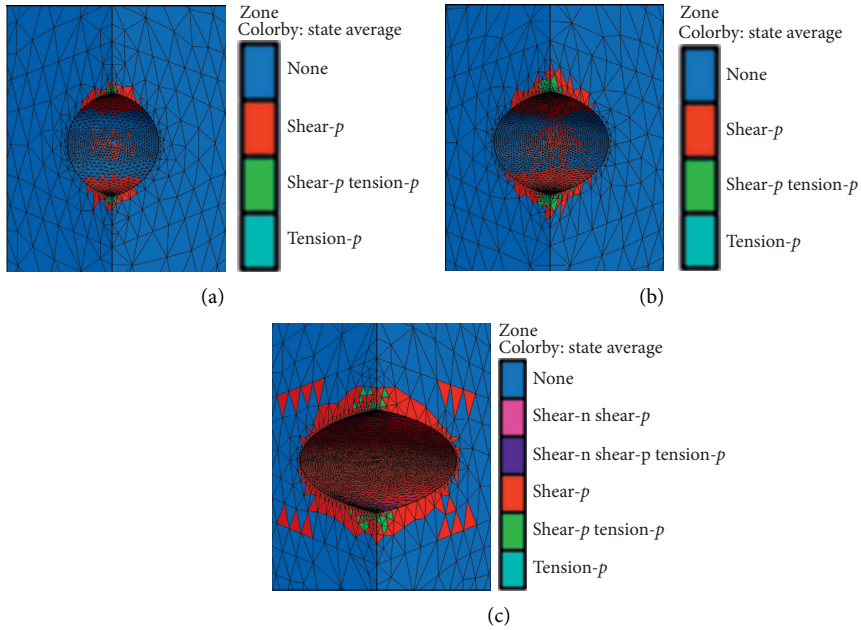

Figure 11: Cloud map of plastic zone distribution of single-cavern horizontal salt rock underground storage with different diameter-to-height ratios ($N = 1.5$, 2.0, and 3.0) (20a). (a) $N = 1.5$; (b) $N = 2.0$; and (c) $N = 3.0$.

and analyzes the influence of the pillar width d on the stability of the salt rock storage. The operation internal pressure is set at 16 MPa, and the pillar width d is set at 40, 60, 80, 100, 120, 140, 160, 180, and 200 m, respectively. Considering that the double-cavern horizontal salt rock storage numerical model is symmetric about the xoz plane, in order to simplify the workload and improve the calculation efficiency, the 1/2 salt rock storage model is established in this section, as shown in Figure 12.

4.1. Vertical and Horizontal Displacement. Through analysis, it can be found that the vertical and horizontal displacement distribution of the double-cavern horizontal salt rock underground storage are basically the same as those of the single-cavern storage. So it is not described here. Figure 13 shows the horizontal displacement distribution cloud map of the double-cavern horizontal salt rock underground storage when the operation time is 20a and the pillar width is 40 m, 80 m, 100 m, 120 m, 140 m, and 180 m.

4.2. Volume Loss Rate. It can be seen from Section 3 that when the diameter-to-height ratio $N = 2.5$, the design capacity of the double-cavern horizontal salt rock underground storage is $2 \times 7.069 \times 10^5\ m^3$. The FISH language is used to process the displacement data of surrounding rock obtained by numerical simulation, and the volume loss rate of the double-cavern horizontal salt rock underground storage under different pillar widths at different operation times can be obtained. Then, take the volume loss rate of the pillar width $d = 200$ m as the standard, and normalize the salt rock storage volume loss rate data under other pillar widths. The curve of the volume loss rate varying with the width of the pillar can be obtained, as shown in Figure 14.

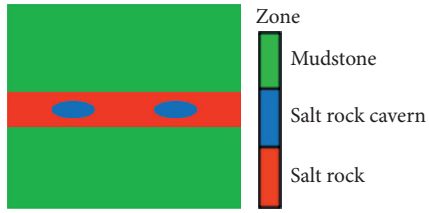

Figure 12: Numerical model of double-cavern horizontal salt rock underground storage ($d = 200$ m).

As can be seen from Figure 14, when the width of the pillar is less than 100 m, the volume loss rate of salt rock storage gradually increases with the increase of pillar width. According to the analysis, when the operation time is 5a and the pillar width is 40 m, the volume loss rate of the salt rock storage is 1.8872%, and when the pillar width increases to 100 m, the volume loss rate of the salt rock storage is 1.8969%. When the width of the pillar is more than 100 m, the influence of pillar width on the volume loss rate of salt rock storage is gradually weakened. The volume loss rate of salt rock storage under different pillar widths ($d = 120$, 140, 160, 180, and 200 m) is always maintained at about 1.9050%. The existence of the pillar between the double cavities is equivalent to imposing a boundary constraint on the cavity from the middle of the pillar. And the larger the pillar width, the weaker the boundary constraint on the cavity. Therefore, when the pillar width is small, the pillar boundary has obvious restraint on the deformation of surrounding rock of double-cavern horizontal salt rock underground storage, so the volume loss rate is small. However, with the increase of pillar width, the restraint of pillar boundary on surrounding rock deformation of salt rock storage is gradually weakened, that is, the volume loss rate increases gradually when the pillar width is larger. With the increase of pillar width, the

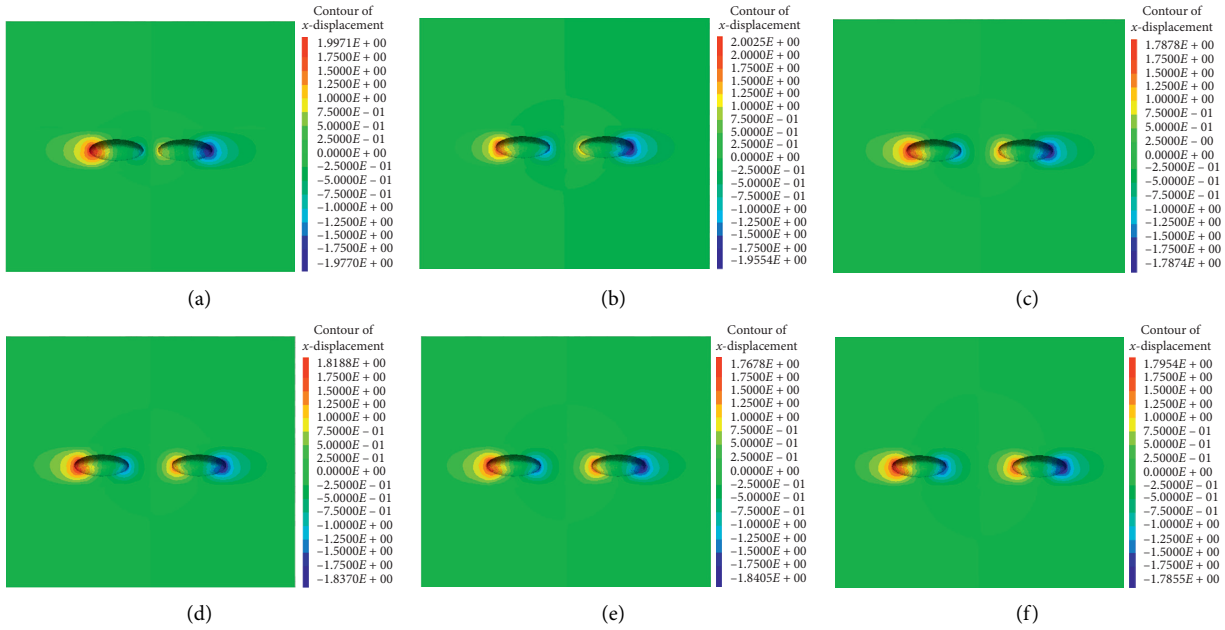

Figure 13: Horizontal displacement distribution cloud map of the double-cavern horizontal salt rock underground storage with different pillar widths (20*a*). (a) $d = 40$ m; (b) $d = 80$ m; (c) $d = 100$ m; (d) $d = 120$ m; (e) $d = 140$ m; and (f) $d = 180$ m.

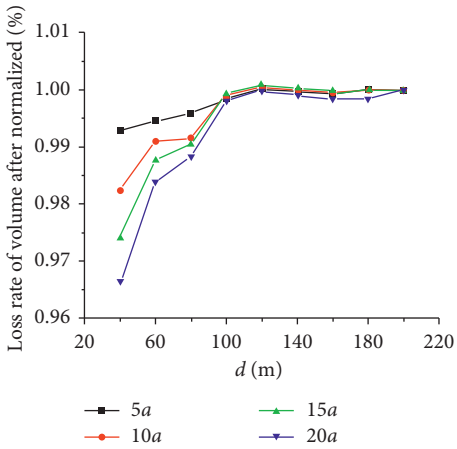

Figure 14: The volume loss rate of the double-cavern horizontal salt rock underground storage varying with the width of the pillar.

influence of pillar width on the volume loss rate of salt rock storage gradually tends to be stable.

Furthermore, compared to the volume loss rate (6.0349%) of a single-cavern horizontal salt rock underground storage with a diameter-to-height ratio $N = 2.5$ after operation for 20*a*, the volume loss rate of the double-cavern horizontal salt rock underground storage under the same conditions after operation for 20*a* is 5.9696%. This indicates that when the pillar width is large enough, the deformation of surrounding rock of double-cavern horizontal salt rock underground storage will still be constrained by the pillar boundary, resulting in the deformation of surrounding rock being restrained to a certain extent and reducing the volume loss rate of salt rock reservoir. Therefore, from the perspective of controlling the volume loss rate of salt rock storage, when the pillar width is greater than 140 m, the mutual influence between the storage cavities gradually weakens.

4.3. Plastic Zone Distribution. When the pillar width is fixed, the change rule of the plastic zone of double-cavern horizontal salt rock underground storage with operation time is basically consistent with that of single-cavern horizontal salt rock underground storage, so it will not be repeated here. Figure 15 shows the plastic zone distribution of the double-cavern horizontal salt rock underground storage when the operation time is 20*a* and the pillar width is 40 m, 80 m, 100 m, 120 m, 140 m, and 180 m. It can be seen that when the width of pillar d is less than 100 m, the interaction between salt rock reservoir cavities is relatively obvious, and a penetrating plastic zone may be formed inside the pillar. When the pillar width exceeds 100 m, as the pillar width increases, the interaction between the salt rock reservoir cavities gradually weakens, and the plastic zones of the surrounding rock of the double-cavern are independent. And the penetrating plastic zone inside the pillar will not be formed. Therefore, from the perspective of the distribution of plastic zones in the surrounding rock of the salt rock storage, the distance between the pillars of the double-cavern horizontal salt rock underground storage should be greater than 100 m.

In addition, it can be found that whether it is a single-cavern or double-cavern horizontal salt rock underground storage through analysis, the surrounding rock stress level during its operation complies with the hydraulic fracturing criterion; that is, the maximum internal pressure does not exceed the minimum principal stress of the surrounding rock of the salt rock storage.

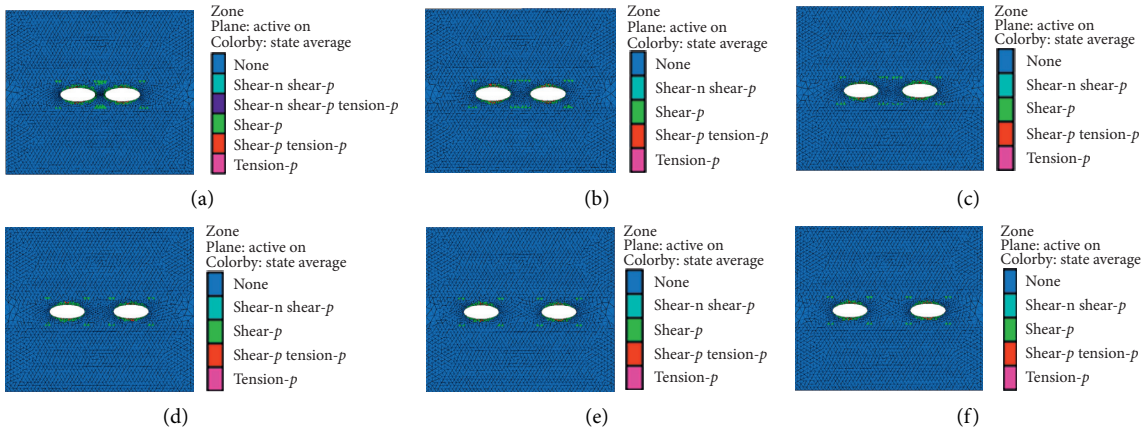

FIGURE 15: Plastic zone distribution map of double-cavern horizontal salt rock underground storage with different pillar widths (20a). (a) $d = 40$ m; (b) $d = 80$ m; (c) $d = 100$ m; (d) $d = 120$ m; (e) $d = 140$ m; and (f) $d = 180$ m.

In summary, for the double-cavern horizontal salt rock underground storage, the greater the width of the pillar, the greater the volume loss rate. Therefore, from the perspective of controlling the volume loss rate, the smaller the pillar width d, the better. However, as the width of the pillar decreases, the interaction between the salt rock storage cavities gradually becomes more obvious. When the pillar width d is more than 100 m, the influence between the cavities gradually weakens. Considering that a certain safety reserve is needed, the pillar width of the double-cavern horizontal salt rock underground storage can be 140 m.

5. Conclusions

For the characteristics of multiple layers and small thickness of the single layer of layered salt rock, the long-term stability of single-cavern horizontal salt rock underground storage with different diameter-to-height ratios is analyzed by using the FLAC^{3D} software, and the optimal diameter-to-height ratio is determined. On this basis, the long-term operation process of the double-cavern horizontal salt rock underground storage is numerically simulated, and the optimal pillar width is obtained. The main conclusions obtained are as follows:

(1) For the single-cavern horizontal salt rock underground storage, the vertical displacement, horizontal displacement, and volume loss rate of salt rock storage increase with the extension of operation time and the increase of diameter-to-height ratio when the diameter-to-height ratio is fixed. When the diameter-to-height is relatively small ($N = 1.5$ and 2.0), the plastic zone of the salt rock storage is smaller and mainly concentrated at the top and bottom of the storage. As the diameter-to-height ratio increases ($N = 2.5$ and 3.0), the plastic zone gradually increases, and the plastic zone is gradually distributed at the interface between mudstone and salt rock, and there is a risk of penetrating the entire salt rock layer.

(2) According to the variation of displacement, volume loss rate, and plastic zone during the operation of salt rock storage, from the perspective of the stability of single-cavern horizontal salt rock underground storage, the smaller the diameter-to-height ratio of the salt rock storage, the better. However, in order to increase the design capacity of the salt rock storage, the diameter-to-height ratio of the storage should be appropriately increased. Therefore, in order to meet both the stability and economic requirements of the salt rock storage, the optimal diameter-to-height ratio of the single-cavern horizontal salt rock underground storage is 2.5.

(3) For the double-cavern horizontal salt rock underground storage, when the width of the pillar is small, the horizontal displacement near the pillar is small, and the horizontal displacement far from the pillar is large. With the increase of the width of the pillar, the distribution of horizontal displacement near the pillar and the distribution of horizontal displacement far away from the pillar tended to be the same. When the width of the pillar is less than 100 m, the interaction between the caverns is obvious, and with the increase of the pillar width, the volume loss rate of the salt rock storage gradually increases. When the width of the pillar exceeds 100 m, the interaction between the caverns gradually weakens, and the influence of pillar width change on the volume loss rate of salt rock storage gradually weakens.

(4) Numerical simulation results of the long-term stability of the double-cavern horizontal salt rock underground storage show that, from the perspective of controlling the volume loss rate of the gas storage, the volume loss rate of the salt rock storage gradually decreases with the decrease of the pillar width; that is, the smaller the pillar width, the better. But when the pillar width is small, the mutual influence between the cavities is more obvious. As the width of the pillar

increases, the interaction between the cavities gradually weakens. Considering that a certain safety reserve is needed, the optimal pillar width of the double-cavern horizontal salt rock underground storage can be 140 m.

Data Availability

The data used to support the findings of this study are available from the corresponding author upon request.

Conflicts of Interest

The authors declare that they have no conflicts of interest.

Acknowledgments

This research was funded by the Housing and Urban-Rural Construction Science and Technology Planning Project of Shaanxi Province (Grant no. 2019-K39) and the Innovation Capability Support Plan of Shaanxi-Innovation Team (Grant no. 2020TD-005).

References

[1] J. Y. Fan, H. P. Xie, J. Chen et al., "Preliminary feasibility analysis of a hybrid pumped-hydro energy storage system using abandoned coal mine goafs," *Applied Energy*, vol. 258, Article ID 114007, 2020.

[2] K. Wu and Z. S. Shao, "Visco-elastic analysis on the effect of flexible layer on mechanical behavior of tunnels," *International Journal of Applied Mechanics*, vol. 11, no. 3, Article ID 1950027, 2019.

[3] J. Chen, H. Peng, J. Fan, X. Zhang, W. Liu, and D. Jiang, "Microscopic investigations on the healing and softening of damaged salt by uniaxial deformation from CT, SEM and NMR: effect of fluids (brine and oil)," *RSC Advances*, vol. 10, no. 5, pp. 2877–2886, 2020.

[4] B. Hu, M. Sharifzadeh, X. T. Feng, W. B. Guo, and R. Talebi, "Roles of key factors on large anisotropic deformations at deep underground excavations," *International Journal of Mining Science and Technology*, vol. 31, no. 2, 2021.

[5] W. Liu, Z. X. Zhang, J. Chen et al., "Feasibility evaluation of large-scale underground hydrogen storage in bedded salt rocks of China: a case study in Jiangsu province," *Energy*, vol. 198, Article ID 117348, 2020.

[6] Z. P. Song, X. X. Tian, Q. Liu, Y. W. Zhang, H. Li, and G. N. Zhou, "Numerical analysis and application of the construction method for small interval tunnel in the turn line of metro," *Science Progress*, vol. 103, no. 3, 2020.

[7] K. Wu, Z. S. Shao, S. Qin, N. Zhao, and H. Hu, "Analytical-based assessment of effect of highly deformable elements on tunnel lining within viscoelastic rocks," *International Journal of Applied Mechanics*, vol. 12, no. 3, Article ID 2050030, 2020.

[8] J. Wang, Q. Zhang, Z. Song, and Y. Zhang, "Creep properties and damage constitutive model of salt rock under uniaxial compression," *International Journal of Damage Mechanics*, vol. 29, no. 6, pp. 902–922, 2020.

[9] J.-B. Wang, X.-R. Liu, Z.-P. Song, and Z.-S. Shao, "An improved Maxwell creep model for salt rock," *Geomechanics and Engineering*, vol. 9, no. 4, pp. 499–511, 2015.

[10] H. Peng, J. Fan, X. Zhang et al., "Computed tomography analysis on cyclic fatigue and damage properties of rock salt under gas pressure," *International Journal of Fatigue*, vol. 134, no. 5, pp. 105523–105532, 2020.

[11] K. Wu, Z. S. Shao, S. Qin, W. Wei, and Z. Chu, "A critical review on the performance of yielding supports in squeezing tunnels," *Tunnelling and Underground Space Technology*, vol. 114, no. 1, 2021.

[12] L. Ma, M. Wang, N. Zhang, P. Fan, and J. Li, "A variable-parameter creep damage model incorporating the effects of loading frequency for rock salt and its application in a bedded storage cavern," *Rock Mechanics and Rock Engineering*, vol. 50, no. 9, pp. 2495–2509, 2017.

[13] S. H. Wang, Q. Z. Wang, J. Xu, and J. L. Ding, "Effect of freeze-thaw on freezing point and thermal conductivity of loess," *Arabian Journal of Geosciences*, vol. 13, no. 5, p. 206, 2020.

[14] J. B. Wang, Q. Zhang, Z. P. Song, Y. W. Zhang, and X. R. Liu, "Mechanical properties and damage constitutive model for uniaxial compression of salt rock at different loading rates," *International Journal of Damage Mechanics*, vol. 30, 2021.

[15] F. Wu, J. Chen, and Q. Zou, "A nonlinear creep damage model for salt rock," *International Journal of Damage Mechanics*, vol. 28, no. 5, pp. 758–771, 2019.

[16] W. Liu, X. Zhang, H. R. Li, and J. Chen, "Investigation on the deformation and strength characteristics of rock salt under different confining pressures," *Geotechnical and Geological Engineering*, vol. 38, no. 4, pp. 5703–5717, 2020.

[17] J. Fan, W. Liu, D. Jiang, J. Chen, W. N. Tiedeu, and J. J. K. Daemen, "Time interval effect in triaxial discontinuous cyclic compression tests and simulations for the residual stress in rock salt," *Rock Mechanics and Rock Engineering*, vol. 53, no. 9, pp. 4061–4076, 2020.

[18] J.-B. Wang, X.-R. Liu, Y.-X. Huang, and X.-C. Zhang, "Prediction model of surface subsidence for salt rock storage based on logistic function," *Geomechanics and Engineering*, vol. 9, no. 1, pp. 25–37, 2015.

[19] J. Chen, C. Du, D. Jiang, J. Fan, and Y. He, "The mechanical properties of rock salt under cyclic loading-unloading experiments," *Geomechanics and Engineering*, vol. 10, no. 3, pp. 325–334, 2016.

[20] J. B. Wang, Q. Zhang, Z. P. Song, and Y. W. Zhang, "Experimental study on creep properties of salt rock under long-period cyclic loading," *International Journal of Fatigue*, vol. 143, Article ID 106009, 2021.

[21] W. Xing, J. Zhao, Z. Hou, P. Were, M. Li, and G. Wang, "Horizontal natural gas caverns in thin-bedded rock salt formations," *Environmental Earth Sciences*, vol. 73, no. 11, pp. 6973–6985, 2015.

[22] G.-c. Liang, X. Huang, X.-y. Peng, Y. Tian, and Y.-h. Yu, "Investigation on the cavity evolution of underground salt cavern gas storages," *Journal of Natural Gas Science and Engineering*, vol. 33, pp. 118–134, 2016.

[23] T. Wang, C. Yang, H. Ma et al., "Safety evaluation of salt cavern gas storage close to an old cavern," *International Journal of Rock Mechanics and Mining Sciences*, vol. 83, pp. 95–106, 2016.

[24] A. Mortazavi and H. Nasab, "Analysis of the behavior of large underground oil storage caverns in salt rock," *International Journal for Numerical and Analytical Methods in Geomechanics*, vol. 41, no. 4, pp. 602–624, 2017.

[25] K. Khaledi, E. Mahmoudi, M. Datcheva, and T. Schanz, "Stability and serviceability of underground energy storage caverns in rock salt subjected to mechanical cyclic loading," *International Journal of Rock Mechanics and Mining Sciences*, vol. 86, pp. 115–131, 2016.

[26] N. Zhang, L. Ma, M. Wang, Q. Zhang, J. Li, and P. Fan, "Comprehensive risk evaluation of underground energy storage caverns in bedded rock salt," *Journal of Loss Prevention in the Process Industries*, vol. 45, pp. 264–276, 2017.

[27] R. Habibi, "An investigation into design concepts, design methods and stability criteria of salt caverns," *Oil and Gas Science and Technology-Revue d IFP Energies Nouvelles*, vol. 74, p. 14, 2019.

[28] W. Liu, Z. Zhang, J. Fan, D. Jiang, and J. J. K. Daemen, "Research on the stability and treatments of natural gas storage caverns with different shapes in bedded salt rocks," *IEEE Access*, vol. 8, pp. 18995–19007, 2020.

[29] J. Q. Deng, Q. Yang, and Y. R. Liu, "Time-dependent behaviour and stability evaluation of gas storage caverns in salt rock based on deformation reinforcement theory," *Tunnelling and Underground Space Technology*, vol. 42, pp. 277–292, 2014.

[30] Y. J. Wang and J. J. Liu, "Critical length and collapse of interlayer in rock salt natural gas storage," *Advances in Civil Engineering*, vol. 2018, Article ID 8658501, 8 pages, 2018.

[31] Z. X. Zhang, D. Y. Jiang, W. Liu et al., "Study on the mechanism of roof collapse and leakage of horizontal cavern in thinly bedded salt rocks," *Environmental Earth Sciences*, vol. 78, no. 2, p. 292, 2019.

[32] C. Yang, W. Jing, J. J. K. Daemen, G. Zhang, and C. Du, "Analysis of major risks associated with hydrocarbon storage caverns in bedded salt rock," *Reliability Engineering & System Safety*, vol. 113, pp. 94–111, 2013.

[33] J. Chen, D. Lu, W. Liu et al., "Stability study and optimization design of small-spacing two-well (SSTW) salt caverns for natural gas storages," *Journal of Energy Storage*, vol. 27, p. 10113, 2020.

[34] Y. F. Kang, J. Y. Fan, D. Y. Jiang, and Z. Z. Li, "Influence of geological and environmental factors on the reconsolidation behavior of fine granular salt," *Natural Resources Research*, vol. 30, 2021.

[35] Z. Chu, Z. Wu, Q. Liu, B. Liu, and J. Sun, "Analytical solution for lined circular tunnels in deep viscoelastic burgers rock considering the longitudinal discontinuous excavation and sequential installation of liners," *Journal of Engineering Mechanics*, vol. 147, no. 8, 2021.

[36] J. B. Wang, X. R. Liu, Z. P. Song, J. Q. Guo, and Q. Q. Zhang, "A creep constitutive model with variable parameters for thenardite," *Environmental Earth Sciences*, vol. 75, no. 6, p. 979, 2016.

[37] Z. P. Song, J. C. Mao, X. X. Tian, Y. W. Zhang, and J. B. Wang, "Optimization analysis of controlled blasting for passing through houses at close range in super-large section tunnels," *Shock and Vibration*, vol. 2019, Article ID 1941436, 16 pages, 2019.

[38] S. Wang, J. Xu, Q. Wang, and D. Cheng, "Modeling of wetting deformation of coarse saline soil with an improved von Wolffersdorff model," *Bulletin of Engineering Geology and the Environment*, vol. 79, no. 9, pp. 4783–4804, 2020.

[39] J.-B. Wang, X.-R. Liu, X.-J. Liu, and M. Huang, "Creep properties and damage model for salt rock under low-frequency cyclic loading," *Geomechanics and Engineering*, vol. 7, no. 5, pp. 569–587, 2014.

[40] K. Wu, Z. S. Shao, and S. Qin, "An analytical design method for ductile support structures in squeezing tunnels," *Archives of Civil and Mechanical Engineering*, vol. 20, p. 91, 2020.

[41] Z. P. Song, Y. Cheng, X. X. Tian, J. B. Wang, and T. T. Yang, "Mechanical properties of limestone from Maixi tunnel under hydro-mechanical coupling," *Arabian Journal of Geosciences*, vol. 13, no. 11, p. 402, 2020.

[42] L. J. Ma, H. F. Xu, M. Y. Wang, and E. B. Li, "Numerical study of gas storage stability in bedded rock salt during the complete process of operation pressure runway," *Chinese Journal of Rock Mechanics Engineering*, vol. 34, no. S2, pp. 4108–4115, 2015.

[43] J. B. Wang, X. R. Liu, Z. P. Song, B. Y. Zhao, B. Jiang, and T. Z. Huang, "A whole process creeping model of salt rock under uniaxial compression based on inverse S function," *Chinese Journal of Rock Mechanics Engineering*, vol. 37, no. 11, pp. 2446–2459, 2018.